Minimal Coordinate Dynamic Simulation Through Singularities

Rohit Kumar, Shivesh Kumar, and Frank Kirchner

Abstract Minimal coordinate formulations generally outperform redundant coordinate approaches for dynamic simulation of multibody systems with kinematic loop-closure constraints. However, they typically require explicit analytical resolution of these constraints, which are not always available. The generalized coordinate partitioning (GCP) method circumvents this limitation by converting easily obtained implicit constraints into explicit ones based on a chosen set of minimal coordinates. Despite its advantages, GCP suffers from singularity issues near critical configurations. This paper presents a minimal-coordinate dynamic formulation for a four-bar mechanism that robustly traverses such singularities by leveraging kinematic tangent cones at singular configurations.

1 Introduction

Multibody systems with closed kinematic loops appear widely in mechanical and robotic applications, and their efficient dynamic simulation remains

---

R. Kumar
Robotics Innovation Center, German Research Center for Artificial Intelligence (DFKI GmbH), Bremen, Germany
e-mail: r.kumar@dfki.de

S. Kumar
Robotics Innovation Center, German Research Center for Artificial Intelligence (DFKI GmbH), Bremen, Germany, and Division of Dynamics, Department of Mechanical Engineering, Chalmers University of Technology, Gothenburg, Sweden
e-mail: kumar@chalmers.se

F. Kirchner
Robotics Innovation Center, German Research Center for Artificial Intelligence (DFKI GmbH), Bremen, Germany
e-mail: frank.kirchner@dfki.de

an important challenge [5]. Although redundantcoordinate formulations are easy to generalize, they require the solving of differential-algebraic equations and often suffer from constraint violation errors and computational inefficiency [1], [2]. Alternative approaches based on augmented Lagrangian formulations have also been explored [9]. Minimal coordinate formulations [4] avoid these drawbacks by analytically eliminating constraints, resulting in smaller and better conditioned systems of equations.

A major obstacle to using minimal coordinates is the need for explicit analytical loopclosure expressions, which can be difficult or impossible to derive for many mechanisms. The generalized coordinate partitioning (GCP) method [10], [3] addresses this issue by converting implicit loopclosure constraints into explicit ones based on a chosen minimal coordinate set. However, GCP becomes unreliable near kinematic singularities, where the mapping between redundant and minimal coordinates loses rank. Robust simulation strategies based on coordinate switching or enhanced constraint enforcement are available [8], but such approaches modify the coordinate representation during simulation, which is undesirable in many contexts. Kinematic singularities are inherent in many mechanisms, such as the classical toggle positions in a fourbar linkage, and robust simulation across these configurations in minimal coordinates without numerical coordinate switching remains an open problem. Recent geometric perspectives show that feasible instantaneous motion directions at singular configurations can be captured by the kinematic tangent cone [7], which coincides with the usual tangent space at regular (smooth) configurations and remains welldefined at singular points where the Jacobian is rankdeficient, thereby generalizing classical Jacobianbased analysis.

In this paper, we leverage this concept to develop a first minimalcoordinate dynamics formulation for the fourbar mechanism that remains valid through singular configurations. Specifically, the kinematic tangent cone is used to construct a consistent velocity mapping within the GCP framework at singular configurations, thereby maintaining well-posed dynamics without coordinate switching. Although demonstrated on a fourbar linkage, the approach may be applicable to broader classes of closedloop systems where singularities arise from non-tangential intersection of motion modes.

2 Preliminaries

Consider a multi-body system with mobility m. After removing the cut/loop joint(s), let n denote the DOF of the spanning tree subjected to n_c constraints. Let $(\mathbf{q}, \dot{\mathbf{q}}, \ddot{\mathbf{q}})$ denote the n-dimensional position, velocity and acceleration vectors for the spanning tree and $(\mathbf{y}, \dot{\mathbf{y}}, \ddot{\mathbf{y}})$ denote the m-dimensional independent position, velocity and acceleration vectors in a regular configuration.

2.1 Loop Closure Constraints

Loop constraints are algebraic constraints on the motion variables of a multi-body system. They can be expressed in implicit $\left(\boldsymbol{\phi}(\mathbf{q}) = \mathbf{0} \in \mathbb{R}^{n_c}\right)$ and explicit $\left(\mathbf{q} = \boldsymbol{\gamma}(\mathbf{y}) \in \mathbb{R}^{n}\right)$ forms which are summarized in Table 1 at position, velocity, and acceleration levels. Here, $\mathbf{K} = \dfrac{\partial \boldsymbol{\phi}}{\partial \mathbf{q}} \in \mathbb{R}^{n_c \times n}$, $\mathbf{k} = -\dot{\mathbf{K}}\dot{\mathbf{q}} \in \mathbb{R}^{n_c}$, $\mathbf{G} = \dfrac{\partial \boldsymbol{\gamma}}{\partial \mathbf{y}} \in \mathbb{R}^{n \times m}$, and $\mathbf{g} = \dot{\mathbf{G}}\dot{\mathbf{y}} \in \mathbb{R}^{n}$. Since $\boldsymbol{\phi}$ and $\boldsymbol{\gamma}$ are equivalent, following can be deduced: $\boldsymbol{\phi} \circ \boldsymbol{\gamma} = \mathbf{0}$, $\mathbf{KG} = \mathbf{0}$, and $\mathbf{Kg} = \mathbf{k}$.

Table 1: Loop constraints [1]

Type	**Position**	**Velocity**	**Acceleration**
implicit	$\boldsymbol{\phi}(\mathbf{q}) = \mathbf{0}$	$\mathbf{K}\dot{\mathbf{q}} = \mathbf{0}$	$\mathbf{K}\ddot{\mathbf{q}} = \mathbf{k}$
explicit	$\mathbf{q} = \boldsymbol{\gamma}(\mathbf{y})$	$\dot{\mathbf{q}} = \mathbf{G}\dot{\mathbf{y}}$	$\ddot{\mathbf{q}} = \mathbf{G}\ddot{\mathbf{y}} + \mathbf{g}$

2.2 Equations of Motion (EOM)

The equations of motion of a constrained mechanical system is given by:

$$\mathbf{M}(\mathbf{q})\ddot{\mathbf{q}} + \mathbf{C}(\mathbf{q}, \dot{\mathbf{q}}) = \boldsymbol{\tau} + \boldsymbol{\tau}_c \tag{1}$$

where $\mathbf{M}(\mathbf{q}) \in \mathbb{R}^{n \times n}$ is the joint space mass-inertia matrix, $\mathbf{C}(\mathbf{q}, \dot{\mathbf{q}}) \in \mathbb{R}^{n \times 1}$ is the vector of coriolis-centrifugal and gravity forces, $\boldsymbol{\tau} \in \mathbb{R}^{n \times 1}$ is the vector of joint forces/torques and $\boldsymbol{\tau}_c \in \mathbb{R}^{n \times 1}$ is the vector of constraint forces due to kinematic loops.

EOM with implicit constraints:

Given implicit loop constraints, $\boldsymbol{\tau}_c = \mathbf{K}^T \boldsymbol{\lambda}$ where $\boldsymbol{\lambda}$ is a vector of unknown forces, also regarded as Lagrangian multipliers. The EOM is a system of $(n + n_c)$ equations in $(n + n_c)$ unknowns given by:

$$\begin{bmatrix} \mathbf{M} & \mathbf{K}^T \\ \mathbf{K} & \mathbf{0} \end{bmatrix} \begin{bmatrix} \ddot{\mathbf{q}} \\ -\boldsymbol{\lambda} \end{bmatrix} = \begin{bmatrix} \boldsymbol{\tau} - \mathbf{C} \\ \mathbf{k} \end{bmatrix}. \tag{2}$$

Forward simulation using (2) requires solving differential algebraic equations (DAEs). It should be noted that implicitly constrainted EOM are easy to setup from readily available CAD data but difficult to solve numerically.

EOM with explicit constraints:

Using Jourdain's principle of virtual power, one could establish that $\mathbf{G}^T\boldsymbol{\tau}_c = \mathbf{0}$. The EOM with explicit constraints is a system of m equations in m unknowns given by:

$$\ddot{\mathbf{y}} = \left(\mathbf{G}^T\mathbf{M}\mathbf{G}\right)^{-1}\mathbf{G}^T\left(\boldsymbol{\tau} - \mathbf{C} - \mathbf{M}\mathbf{g}\right). \tag{3}$$

Forward simulation using (3) requires solving ordinary differential equations (ODEs). Note that explicitly constrained EOM are difficult to setup (γ-map and derivatives) but easy to solve numerically (for e.g., using Runge-Kutta method).

Generalized Coordinate Partitioning (GCP):

The γ-mapping and its derivatives are sometimes complicated trigonometric functions and difficult to derive. The GCP method splits redundant coordinates $\mathbf{q}$ into independent $\mathbf{y}$ and dependent coordinates $\mathbf{q}_d$ and computes $\mathbf{G}$ and $\mathbf{g}$ from $\mathbf{K}$ and $\mathbf{k}$, which are easier to derive [10]. The γ-mapping itself can then be numerically computed with the NewtonRaphson method. The quantities $\mathbf{G}$ and $\mathbf{g}$ can be obtained as follows

$$\mathbf{G} = \begin{pmatrix} \mathbf{I} \\ -\mathbf{K}_d^{-1}\mathbf{K}_i \end{pmatrix}, \qquad \mathbf{g} = \begin{pmatrix} \mathbf{0} \\ \mathbf{K}_d^{-1}\mathbf{k} \end{pmatrix}. \tag{4}$$

Forward simulation can then be achieved in minimal coordinates using (3).

2.3 Singularities

The finite motion of the system is uniquely determined by the geometry of the configuration space - the solution variety $V := \boldsymbol{\phi}^{-1}(\mathbf{0})$ and the local finite DOF of the system at configuration $\mathbf{q} \in V$ is the dimension of V (i.e., $\delta_{\text{loc}} = \dim_{\mathbf{q}}V$). The corresponding velocity constraints $\mathbf{K}(\mathbf{q})\dot{\mathbf{q}} = \mathbf{0}$ determine the vector space of feasible first-order motions $K^1_{\mathbf{q}} := \ker\mathbf{K}(\mathbf{q})$. The differential/instantaneous DOF of the system at $\mathbf{q} \in V$ is $\delta_{\text{diff}}(\mathbf{q}) = \dim K^1_{\mathbf{q}}$. A configuration $\mathbf{q} \in V$ is a *kinematic singularity* if and only if δ_{diff} is not constant in the neighborhood of $\mathbf{q}$ in V. Otherwise, $\mathbf{q}$ is a regular configuration. The point $\mathbf{q}$ in V is a *c-space singularity* if and only if V is not a smooth manifold at $\mathbf{q}$.

Within the GCP framework, singularities arise when the dependent coordinate Jacobian matrix $\mathbf{K}_d$ becomes singular or loses rank. Since explicit constraint map and its derivatives are constructed through inversion of $\mathbf{K}_d$, singular configurations correspond to configurations at which $\det(\mathbf{K}_d) = 0$.

At such configurations, the matrices $\mathbf{G}$ and $\mathbf{g}$ become undefined, and (3) in minimal coordinates cannot be constructed. In practice, when starting the simulation in a regular configuration, the mechanism may pass through the singularity with an unpredictable switch of operation modes subject to the choice of time step size.

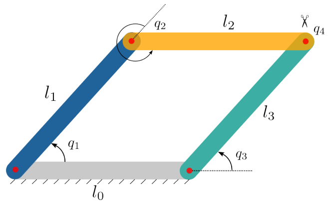

(a) Four-bar mechanism

(b) Singular configuration $q_1 = q_3 = 0$

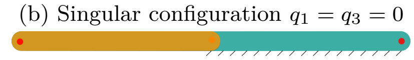

(c) Singular configuration $q_1 = q_3 = \pi$

Fig. 1: Four-bar mechanism and its singular configurations

3 Robust GCP Through Singularity

We propose to modify the GCP method to make it robust to the crossing of singularity. The method is explained here with the help of a four bar mechanism where singularities arise from non-tangential intersection of motion modes. Consider the four bar mechanism in Fig. 1a with the link l_0 fixed to the ground and it's two singular configurations in Fig. 1b & 1c. Assuming q_4 to be the cut joint, the spanning tree joint coordinate position vector is written as $\mathbf{q} = (q_1, q_2, q_3)^T$. Given the mechanism is planar, the cut joint imposes $n_c = 2$ independent position constraints given by:

$$\boldsymbol{\phi}(\mathbf{q}) = \begin{bmatrix} l_1 \cos q_1 + l_2 \cos q_{12} - l_0 - l_3 \cos q_3 \\ l_1 \sin q_1 + l_2 \sin q_{12} - l_3 \sin q_3 \end{bmatrix} = \mathbf{0}_{2\times 1} \tag{5}$$

where $q_{12} = q_1 + q_2$. The implicit constraint Jacobian $\mathbf{K} \in \mathbb{R}^{2\times 3}$ is given by:

$$\mathbf{K} = \begin{bmatrix} -l_1 \sin q_1 - l_2 \sin q_{12} & -l_2 \sin q_{12} & l_3 \sin q_3 \\ l_1 \cos q_1 + l_2 \cos q_{12} & l_2 \cos q_{12} & -l_3 \cos q_3 \end{bmatrix} \tag{6}$$

To make the analysis even simpler, consider a rhombus variant of the 4-bar mechanism i.e., $l_0 = l_1 = l_2 = l_3 = 1$. Fig. 2 shows the three operation modes of this mechanism. For the purpose of GCP, assume $y = q_1$ is our independent coordinate and $\mathbf{q}_d = (q_2, q_3)^T$ is the set of dependent coordinates when starting from a regular configuration in operation mode shown in Fig. 2a i.e. $q_1 \neq 0$ and $q_3 \neq \pi$. For example, starting at a regular configuration $y = 0.2$ and thus $q = (0.2, -0.2, 0.2)^T$ at $t = 0.0$, the implicit constraint

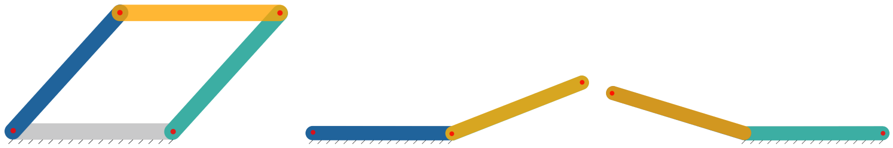

(a) $q_1 = -q_2 = q_3$ (b) $q_1 = 0, q_2 = q_3$ (c) $q_3 = \pi, q_2 = -\pi$

Fig. 2: Operation modes of the four bar mechanism with $l_0 = l_1 = l_2 = l_3$

Jacobian takes the value:

$$\mathbf{K} = \begin{bmatrix} -0.1987 & 0 & 0.1987 \\ 1.9801 & 1 & -0.9801 \end{bmatrix} \quad \text{with} \quad \mathrm{rank}(\mathbf{K}) = 2 \quad \text{and} \quad \mathrm{rank}(\ker\mathbf{K}) = 1.$$

In this configuration, $\mathbf{G}$ can be derived from $\mathbf{K}$ using (4) and equals $\mathbf{G} = (1, -1, 1)^T$ which is a constant. Thus the bias acceleration term vanishes, i.e., $\mathbf{g} = \mathbf{0}$, and the joint accelerations are simply related to the independent acceleration by $\ddot{\mathbf{q}} = \mathbf{G}\ddot{\mathbf{y}}$. At the critical configuration $\mathbf{q}^* = (0, 0, 0)^T$, the implicit constraint Jacobian and its null space take the value:

$$\mathbf{K} = \begin{bmatrix} 0 & 0 & 0 \\ 2 & 1 & -1 \end{bmatrix} \,\&\, \mathrm{rank}(\mathbf{K}) = 1, \ker(\mathbf{K}) = \begin{bmatrix} -0.577 & 0.0 \\ 0.577 & 0.707 \\ -0.577 & 0.707 \end{bmatrix} \,\&\, \mathrm{rank}(\ker\mathbf{K}) = 2.$$

Since there is a change in rank of the $\ker(\mathbf{K})$ in the vicinity of the critical configuration i.e. δ_{diff} is not constant, the mechanism passes through a kinematic singularity. Through higher order local analysis of this configuration, it has been shown that the tangent space $T_{\mathbf{q}^*}V = \mathrm{span}\, C_{\mathbf{q}^*}V$ is the two dimensional vector space identical to $K^1_{\mathbf{q}^*}$ [6]. Since, the tangent space is not identical to the tangent cone in this case i.e., $T_{\mathbf{q}^*}V \neq C_{\mathbf{q}^*}V$, it is also a c-space singularity. When it comes to GCP, the matrix $\mathbf{K}_d$ loses its rank and (4) can not be used to compute $\mathbf{G}$. In order to derive $\mathbf{G}$, we use the tangent space $T_{\mathbf{q}^*}$.

$$\mathbf{G} = \ker(\mathbf{K})\boldsymbol{\alpha} \quad \text{with} \quad \boldsymbol{\alpha} = (\ker(\mathbf{K}))^\dagger\, \dot{\mathbf{q}}_{i-1}. \tag{7}$$

Using (7) at this critical configuration, we get $\boldsymbol{\alpha} = \left(-1/\sqrt{3}, 0\right)^T$ and $\mathbf{G} = (1, -1, 1)^T$. This choice ensures that the simulation continues on the same operation mode where we started with. Similarly, at the next critical configuration $\mathbf{q}^* = (\pi, -\pi, \pi)^T$, the implicit constraint Jacobian and its null space take the value:

$$\mathbf{K} = \begin{bmatrix} 0 & 0 & 0 \\ 0 & 1 & 1 \end{bmatrix} \,\&\, \mathrm{rank}(\mathbf{K}) = 1, \ker(\mathbf{K}) = \begin{bmatrix} 0.8165 & 0.5774 \\ 0.4082 & -0.5774 \\ -0.4082 & 0.5774 \end{bmatrix} \,\&\, \mathrm{rank}(\ker\mathbf{K}) = 2.$$

Fig. 3 shows the tangent space of this critical configuration and the possible

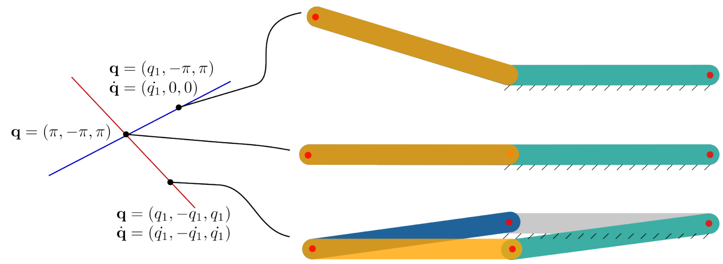

Fig. 3: Kinematic tangent space (red and blue denotes different operation modes)

switch in operation mode that may occur in this configuration. Again using (7) at this critical configuration, we get $\boldsymbol{\alpha} = \left(0, \sqrt{3}\right)^T$ and $\mathbf{G} = (1, -1, 1)^T$ and the simulation continues on the same operation mode where we started with.

Remarks:

It is assumed that the simulation starts in a regular configuration where $\mathbf{q}$ is well-defined. (7) is valid for single DOF mechanisms but maybe extended to multi-DOF kinematic loops and is outside the scope of the paper. Even though staying in the same operation mode requires the knowledge of the configuration velocity in previous time step $\dot{\mathbf{q}}_{i-1}$ in (7), the expression behaves well for small velocities as long as the direction information is well-contained. Being a minimal coordinate algorithm, this is a valid assumption.

4 Results

This section presents the results of forward dynamic simulations of the 4-bar mechanism in free fall. The equations of motion in explicit form Eq. (3) are integrated over a duration of 5s using a fourth-order Runge-Kutta scheme with a fixed time step of 0.001s.

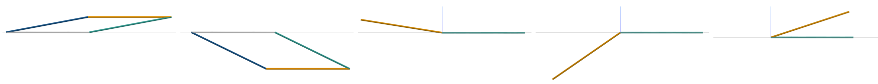

1. $t = 0.0s$ 2. $t = 1.0s$ 3. $t = 1.6s$ 4. $t = 3.0s$ 5. $t = 3.6s$

(a) GCP: Operation mode switching randomly due to numerics

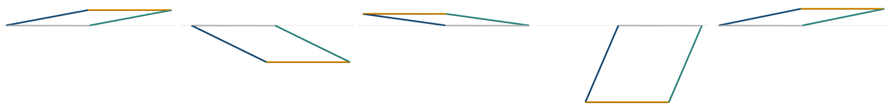

1. $t = 0.0s$ 2. $t = 1.0s$ 3. $t = 1.6s$ 4. $t = 3.0s$ 5. $t = 3.6s$

(b) *Proposed:* Same operation mode

Fig. 5: Forward dynamics simulation results in minimal coordinates

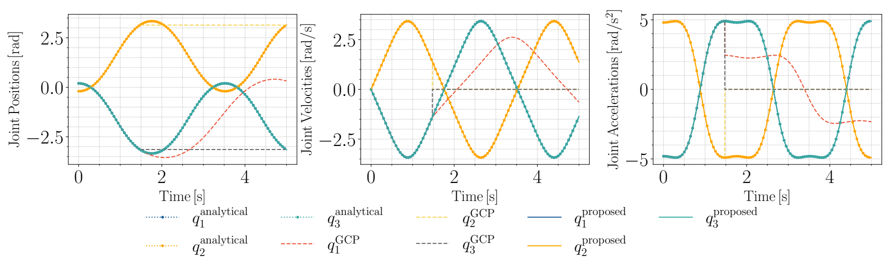

Fig. 4: Joint positions, velocities, accelerations of all joints (legend identifiers are consistent across the three subplots for each joint coordinate)

Fig. 4 compares the joint positions, velocities, and accelerations obtained using three different approaches. The *analytical* solution corresponds to the use of symbolic expressions for $\gamma(y)$ and $\mathbf{G}$, which serves as a reference. The *GCP* approach denotes the classical generalized coordinate partitioning method and the *proposed* refers to robust GCP method which does not arbitrarily switches between operation modes. As shown in Fig. 4, when the mechanism reaches the singular configuration at $q_1 = -\pi$, the GCP formulation leads to numerical locking. In this case, joint q_2 and q_3 remain constant in position, and their velocities and accelerations abruptly drop to zero, following the operation mode in Fig. 2c. The behavior is non physical as the mechanism effectively becomes immobilized despite the presence of gravity, indicating a failure of the formulation to correctly handle singular configurations. A visual comparison of the free fall simulation in the two cases in shown in Fig. 5.

We validate the proposed approach again by considering a variant of the parallelogram linkage with equally opposite link lengths, such that $(l_0 = l_2) < (l_1 = l_3)$. The mechanism starts in the same operation mode as before.

Figure 6 and Fig. 7 show the comparison in joint space and visual animation respectively.

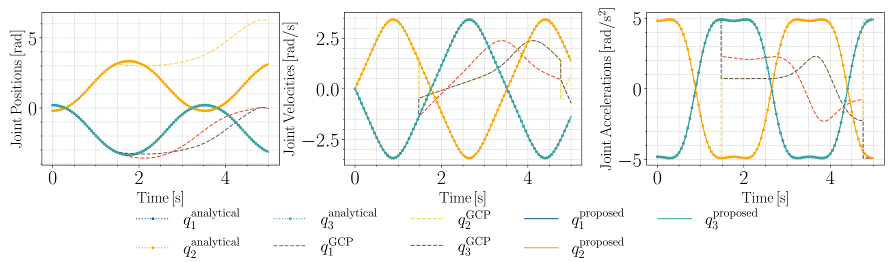

Fig. 6: Joint positions, velocities, accelerations of all joints (legend identifiers are consistent across the three subplots for each joint coordinate)

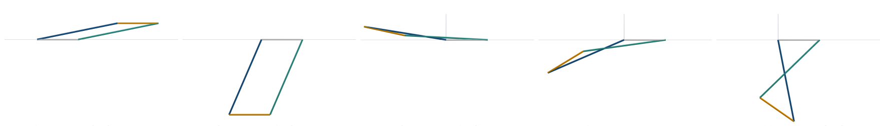

1. $t = 0.0s$ 2. $t = 1.0s$ 3. $t = 1.6s$ 4. $t = 3.0s$ 5. $t = 3.6s$

(a) GCP: Operation mode switching randomly due to numerics

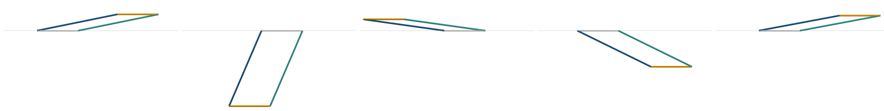

1. $t = 0.0s$ 2. $t = 1.0s$ 3. $t = 1.6s$ 4. $t = 3.0s$ 5. $t = 3.6s$

(b) *Proposed:* Same operation mode

Fig. 7: Forward dynamics simulation results in minimal coordinates

5 Conclusion

This paper introduced a minimal coordinate formulation for forward dynamic simulation of a four bar mechanism, addressing non-physical behavior at kinematic singularities. By explicitly exploiting the null space of the constraint Jacobian and enforcing the consistency of admissible tangential directions, the proposed approach prevents spurious operation-mode switching and numerical locking observed in conventional generalized coordinate partitioning. Free-fall simulations of a rhombus and parallelogram mechanisms demonstrated exact agreement with analytical solutions, while standard GCP exhibited discontinuities in velocities and accelerations at singular configurations.

Future work will focus on extending the proposed formulation to more general kinematic mechanisms with higher degrees of freedom and more complex singularity structures.

Acknowledgements The first author acknowledges the support of CoEx project (Grant Number 01IW24008) funded by the German Aerospace Center with federal funds from the Federal Ministry for Research, Technology and Aeronautics. The second author acknowledges the support of the Wallenberg AI, Autonomous Systems and Software Program (WASP) funded by the Knut and Alice Wallenberg Foundation.

References

1. Featherstone, R.: Rigid Body Dynamics Algorithms. Springer US, Boston, MA (2008)
2. Jain, A.: Robot and multibody dynamics: analysis and algorithms. Springer Science & Business Media (2010)
3. Kumar, R., Kumar, S., Müller, A., Kirchner, F.: Modular and hybrid numerical-analytical approach-a case study on improving computational efficiency for series-parallel hybrid robots. In: 2022 IEEE/RSJ International Conference on Intelligent Robots and Systems (IROS), pp. 3476–3483. IEEE (2022)
4. Kumar, S., Szadkowski, K.A.v., Mueller, A., Kirchner, F.: An analytical and modular software workbench for solving kinematics and dynamics of series-parallel hybrid robots. Journal of Mechanisms and Robotics **12**(2), 021114 (2020)
5. Kumar, S., Wöhrle, H., de Gea Fernández, J., Müller, A., Kirchner, F.: A survey on modularity and distributivity in series-parallel hybrid robots. Mechatronics **68**, 102367 (2020)
6. Müller, A.: Local kinematic analysis of closed-loop linkagesmobility, singularities, and shakiness. Journal of Mechanisms and Robotics **8**(4), 041013 (2016)
7. Müller, A.: Kinematic tangent cone – a useful concept for the local mobility and singularity analysis. In: T. Uhl (ed.) Advances in Mechanism and Machine Science, pp. 337–346. Springer International Publishing, Cham (2019)
8. Pappalardo, C.M.: A natural absolute coordinate formulation for the kinematic and dynamic analysis of rigid multibody systems. Nonlinear Dynamics **81**, 1841–1869 (2015). URL https://api.semanticscholar.org/CorpusID:117634252
9. Ruggiu, M., Frau, E., Rea, P.: Forward dynamics of the five-bar parallel mechanism in presence of singularities. In: D.D. Cioboată (ed.) International Conference on Reliable Systems Engineering (ICoRSE) - 2022 (2023)
10. Wehage, R.A., Haug, E.J.: Generalized coordinate partitioning for dimension reduction in analysis of constrained dynamic systems. Journal of Mechanical Design **104**(1), 247–255 (1982)